The Role of the Southern Ocean in Uptake and Storage of Anthropogenic Carbon Dioxide

Ken Caldeira* and Philip B. Duffy

An ocean-climate model that shows high fluxes of anthropogenic carbon dioxide into the Southern Ocean, but very low storage of anthropogenic carbon there, agrees with observation-based estimates of ocean storage of anthropogenic carbon dioxide. This low simulated storage indicates a subordinate role for deep convection in the present-day Southern Ocean. The primary mechanism transporting anthropogenic carbon out of the Southern Ocean is isopycnal transport. These results imply that if global climate change reduces the density of surface waters in the Southern Ocean, isopycnal surfaces that now outcrop may become isolated from the atmosphere, tending to diminish Southern Ocean carbon uptake.

There has been considerable debate (*1, 2*) about the importance of Southern Ocean uptake of anthropogenic CO_2. Several modeling studies (*2–6*) have indicated a relatively large Southern Ocean sink for anthropogenic CO_2. Until recently, it was impossible to test these and related model predictions against observation-based estimates of local concentrations of anthropogenic carbon in the ocean, because of the difficulty of distinguishing anthropogenic carbon from naturally occurring carbon. However, a recently developed technique (*7*) allows the anthropogenic component of ocean CO_2 to be estimated from observations. Applications of this and similar techniques (*2, 8, 9*) indicate relatively little storage of anthropogenic CO_2 in the Southern Ocean, with the primary locus of Southern Hemisphere carbon storage occurring in the Subtropical Convergence. Observationally based estimates (*2, 8*) suggest that column inventories in the Southern Ocean are among the lowest in the world ocean. From this, it has been inferred that fluxes of anthropogenic CO_2 into the Southern Ocean are small (*2*). Our model results show that fluxes into the Southern Ocean are relatively high, but storage is low because anthropogenic carbon entering the Southern Ocean is transported northward isopycnally into the Subtropical Convergence.

To study the problem of carbon uptake and storage in the Southern Hemisphere, we used an extensively modified version (*10*) of the Geophysical Fluid Dynamics Laboratory (GFDL) Modular Ocean Model (*11*). The model domain was global, with 90 grid points in the longitudinal and latitudinal directions and 23 levels in the vertical. The dynamic/thermodynamic sea ice model used here is a parallel version of the model of Oberhuber (*12*). In our simulation, as in earlier simulations (*10, 13*), salt rejected during the formation of sea ice is instantaneously mixed into the subsurface ocean. The maximum depth of mixing is calculated on the basis of a prescribed density contrast relative to the surface (*13*). The motivation for instantaneous mixing of rejected salt is that brine rejected during sea ice formation in the real ocean typically sinks convectively to the bottom of the mixed layer (*14*). Earlier work (*10*) showed that instantaneous mixing of rejected salt into the subsurface ocean dramatically improves simulated salinity and chlorofluorocarbon-11 (CFC-11) in the Southern Ocean in our model. As described in (*10*), our model uses seasonally varying surface fluxes of momentum, fresh water, and heat.

The perturbation CO_2 calculation (*5*) presented here was performed assuming no long-term changes in ocean circulation or in biological transport of carbon within the ocean (*6, 15*). The fundamental assumption behind this perturbation calculation is that the marine carbon cycle is separable into two nearly linear tracer transport problems: the natural carbon cycle and the anthropogenic perturbation. The biological surface-to-deep-ocean transport of carbon "drops out" of the perturbation calculation for anthropogenic CO_2 because the biological carbon pump is assumed not to be directly affected by the anthropogenic carbon perturbation; i.e., we assume that there is no biological transport of anthropogenic carbon. For purposes of calculating air-sea exchange of anthropogenic CO_2, gas transfer velocities were made a function of wind speed (*16*).

Temperature and salinity fields in our simulation were initialized from the Levitus climatology (*17*). In order to speed the approach of the solution to equilibrium, we used an acceleration technique (*18*) in which longer time steps are used in the deeper model layers. The simulation was "spun up" for 1500 surface years, equivalent to 11,250 years in the deepest model layer, and then run for another 500 years without deep-ocean acceleration. At this point, simulations of transient tracers (CFC-11 and anthropogenic CO_2) were begun.

Our model simulates important aspects of the inferred distributions of anthropogenic

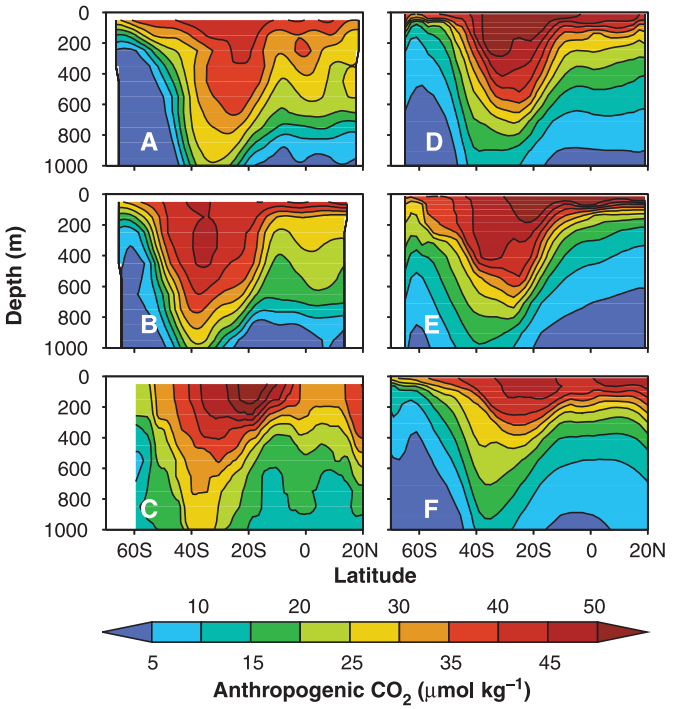

Fig. 1. Latitude-depth sections showing estimated concentrations of anthropogenic CO_2. (**A**) and (**D**) are in the Indian Ocean at ~57°E in 1995; (**B**) and (**E**) are for ~92°E in 1995. (**C**) and (**F**) show the western Atlantic in 1989. (A through C) Anthropogenic CO_2 concentrations inferred from ocean tracer observations for the Indian (*2*) and Atlantic (*8*) oceans. (D through F) Our model results for those same sections. Both estimates show relatively little anthropogenic CO_2 in the Southern Ocean, with the deepest penetration of anthropogenic CO_2 between 30° and 40°S.

Climate System Modeling Group, Lawrence Livermore National Laboratory, Livermore, CA 94550, USA.

*To whom correspondence should be addressed. E-mail: kenc@llnl.gov

carbon in the Indian and Atlantic oceans. Latitude-depth sections in the Indian Ocean (Fig. 1) show generally good agreement between simulated and observation-based estimates of anthropogenic carbon concentrations. Our model results confirm the conclusions of Sabine *et al.* (*2*) that little anthropogenic carbon is stored in the Southern Ocean and that the highest column inventories in the Indian Ocean are associated with the Subtropical Convergence between 30° and 40°S. Furthermore, analysis of our results along isopycnal surfaces confirms their conclusion that "the primary pathway for CO_2 to enter the ocean's interior is from movement along isopycnals" (*2*, p. 191). The most notable disagreement between the simulated and observation-based estimates in these sections is in the northern Indian Ocean. Assuming that the observation-based estimates are correct in this region, the model apparently upwells too strongly, resulting in insufficiently deep penetration of anthropogenic carbon there.

Our simulated column inventories (vertically integrated concentrations) of anthropogenic carbon (Fig. 2) in the Indian Ocean also agree well with those inferred by Sabine *et al.* (*2*). In the observation-based data, column inventories near the Antarctic continent range from <10 to ~20 mol m^{-2}. Model values here are generally <20 mol m^{-2}, but reach values of <10 mol m^{-2} at only one grid point. Farther north, both model and data show maximum column inventories of 30 to 50 mol m^{-2} occurring between latitudes of 30° and 40°S. In the northern Indian Ocean, column inventories decrease to between 20 and 30 mol m^{-2} in the data. Our model results are somewhat lower (typically between 10 and 20 mol m^{-2}), an apparent consequence of excessive simulated upwelling in this region.

Observation-based estimates (*8*) of anthropogenic CO_2 concentrations in the Atlantic Ocean are unavailable south of ~65°S; nonetheless, the model- and observation-based estimates suggest very low storage of anthropogenic carbon in the Atlantic sector of the Southern Ocean north of 65°S. The observation-based sections (Fig. 1) show lines of constant anthropogenic carbon concentrations sloping sharply upward south of ~40°S; thus, column inventories decrease from north to south in this region. The model-based estimates (Figs. 1 and 2) show these same patterns (although simulated values are typically lower than the observation-based values). Near Antarctica, our simulated column inventories are among the lowest in the simulated ocean.

The model used here also gives realistic representations of salinity and CFC-11 in the Southern Ocean (*10*), which are often simulated poorly in this region. Thus, our simulations, together with a variety of tracer observations (*2, 8, 19*), point to low storage of anthropogenic carbon in the Southern Ocean. Despite the reduced Southern Ocean storage in our simulation relative to others, our global simulated ocean uptake of 1.99 Pg of anthropogenic carbon in 1990 agrees well with previous estimates of 2.0 ± 0.5 Pg of carbon per year for the 1980s (*4*).

Our model results show that maximum fluxes of anthropogenic carbon into the Southern Ocean occur farther south than maximum column inventories (Figs. 2 and 3). This happens because anthropogenic carbon, which enters isopycnal surfaces outcropping in the Southern Ocean, is transported northward along those surfaces to the Antarctic Convergence (*2, 8*). In the Southern Ocean, inferred (*2, 8*) and simulated anthropogenic carbon concentrations decrease to the north as isopycnal surfaces deepen, and isopycnals that are not ventilated have low anthropogenic CO_2 concentrations; this indicates that isopycnal processes dominate anthropogenic carbon transport in this region (*2, 8*). Simulated air-to-sea fluxes are greatest in the Southern Ocean when isopycnal surfaces are ventilated during wintertime deepening of the mixed layer.

A recent modeling study (*6*) concluded that one result of global warming could be to increase the vertical stability in the Southern Ocean, largely "shutting down" deep convective activity in that region. Broecker *et al.* (*20*) suggested that most of this "shut down" of Southern Ocean convective activity may have occurred already, on the basis of data indicating that ventilation of the deep South-

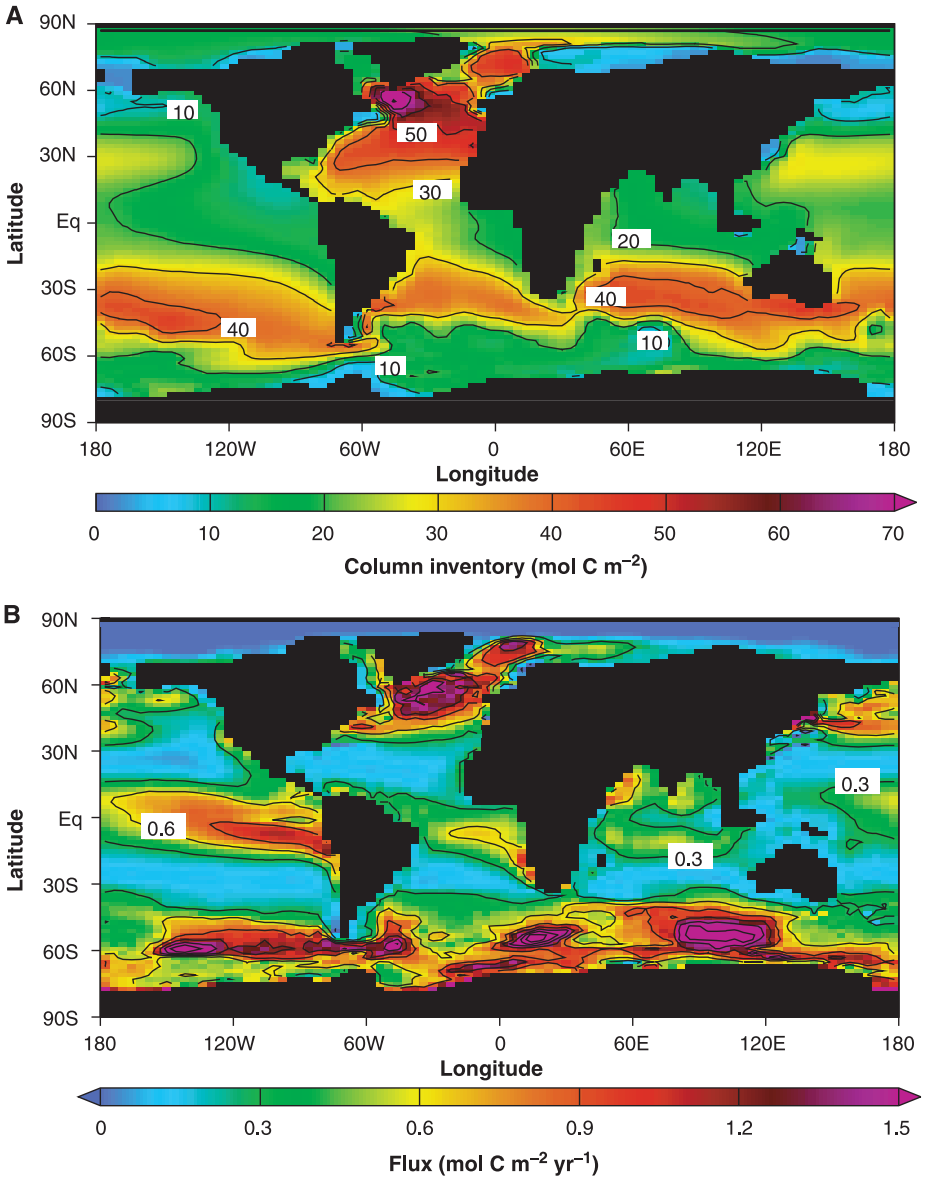

Fig. 2. (**A**) Column inventories and (**B**) fluxes of anthropogenic carbon as of 1995, as simulated by the Lawrence Livermore National Laboratory model. Maximum Southern Hemisphere carbon storage occurs in the Antarctic Convergence, whereas fluxes are highest in the Southern Ocean.

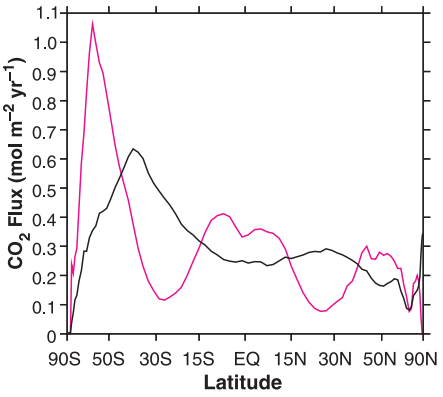

Fig. 3. Zonal mean anthropogenic CO_2 accumulation rate in the ocean (black line) and zonal mean anthropogenic CO_2 flux into the ocean (magenta line), by latitude band (averaged over land and ocean areas for 1995). The latitude axis is scaled so that equal horizontal distances represent equal areas on Earth's surface. On this scale, the total flux or accumulation into the ocean is proportional to the area under the appropriate curve. The Southern Ocean is an area with the highest anthropogenic CO_2 fluxes, but the Antarctic Convergence is the area with the largest anthropogenic CO_2 accumulation.

ern Ocean was much more vigorous in the period from ~1350 to 1880 A.D. than in the recent past. Our simulations reflect primarily late–20th century oceanographic conditions and support the conclusion of a subordinate role for deep convection in the Southern Ocean during this time period (*21*).

Our conclusion that present-day Southern Ocean uptake of anthropogenic carbon is large, but Southern Ocean storage is relatively small, has implications for the mechanisms governing future changes in the ocean carbon cycle. If most of the anthropogenic carbon entering the Southern Ocean is being transported northward isopycnally to the Antarctic Convergence, then a reduction in deep convection would have little impact on Southern Ocean uptake of anthropogenic carbon. Thus, the particular scenario described in (*6*) seems unlikely to occur. Changes in ocean circulation, reduction in sea ice coverage, temperature-dependent changes in CO_2 solubility, and changes in biological activity will impact oceanic CO_2 uptake (*6, 15*). Nevertheless, if global climate change reduces the density of surface waters in the Southern Ocean (*6, 15*), isopycnal surfaces that are now ventilated would become isolated from the atmosphere; this would tend to diminish Southern Ocean carbon uptake.

References and Notes

1. J. L. Sarmiento and E. T. Sundquist, *Nature* **356**, 589 (1992); C. D. Keeling, S. C. Piper, M. Heimann, in *Aspects of Climate Variability in the Pacific and Western Americas*, vol. 55 of *Geophysical Monograph Series*, D. H. Peterson, Ed. (American Geophysical Union, Washington, DC, 1989), pp. 305–363; P. P. Tans, I. Y. Fung, T. Takahashi, *Science* **247**, 1431 (1990).
2. C. L. Sabine *et al.*, *Global Biogeochem. Cycles* **13**, 179 (1999).
3. E. Maier-Reimer and K. Hasselmann, *Clim. Dyn.* **2**, 63 (1987).
4. U. Siegenthaler and J. L. Sarmiento, *Nature* **365,** 119 (1993).
5. J. L. Sarmiento, J. C. Orr, U. Siegenthaler, *J. Geophys. Res.* **97**, 3621 (1992); J. L. Sarmiento, C. Le Quere, S. W. Pacala, *Global Biogeochem. Cycles* **9**, 121 (1995).
6. J. L. Sarmiento, T. M. C. Hughes, R. J. Stouffer, S. Manabe, *Nature* **393**, 245 (1998).
7. N. Gruber, J. L. Sarmiento, T. S. Stocker, *Global Biogeochem. Cycles* **10,** 809 (1996).
8. N. Gruber, *Global Biogeochem. Cycles* **12**, 165 (1998).
9. A. Poisson and C.-T. Chen, *Deep Sea Res. Part A* **34**, 1255 (1987); P. P. Murphy, R. A. Freely, R. H. Gammon, K. C. Kelly, L. S. Waterman, *Mar. Chem.* **35**, 77 (1991).
10. P. B. Duffy and K. Caldeira, *Geophys. Res. Lett.* **24**, 1323 (1997); K. Caldeira and P. B. Duffy, *Geophys. Res. Lett.* **25**, 1003 (1998). Our simulations tend to have slow and shallow North Atlantic Deep Water, but they represent the Southern Ocean relatively well.
11. R. Pacanowski, K. Dixon, A. Rosati, *The G.F.D.L. Modular Ocean Model Users Guide version 1.0, GFDL Ocean Group Technical Report 2* (NOAA/Geophysical Fluid Dynamics Laboratory, Princeton, NJ, 1991).
12. J. M. Oberhuber, *J. Phys. Oceanogr.* **23**, 808 (1993).
13. P. B. Duffy, M. Eby, A. J. Weaver, *Geophys. Res. Lett.* **26**, 1739 (1999).
14. D. G. Martinson, *J. Geophys. Res.* **95**, 11641 (1990). The horizontal sizes of regions of brine-induced convection are very small in comparison to the grid cells in our model. Thus, a first-order representation of this subgrid-scale convection process is to sink rejected salt without mixing other tracers (*10, 13*).
15. F. Joos, G.-K. Plattner, T. F. Stocker, O. Marchal, A. Schmittner, *Science* **284**, 464 (1999); R. J. Matear and A. C. Hirst, *Tellus Ser. B* **51**, 722 (1999).
16. R. Wanninkhof, *J. Geophys. Res.* **97**, 7373 (1992).
17. S. Levitus and T. P. Boyer, *Temperature*, vol. 4 of *World Ocean Atlas 1994*, *NOAA Atlas NESDIS 4* (National Oceanographic Data Center, Silver Spring, MD, 1994).
18. K. Bryan, *J. Phys. Oceanogr.* **14**, 666 (1984).
19. Evidence of deep penetration of CFCs in the Southern Ocean [A. H. Orsi, G. C. Johnson, J. L. Bullister, *Prog. Oceanogr.* **43**, 55 (1999)] may appear to contradict the conclusions drawn here. However, CFCs equilibrate with the atmosphere much more rapidly than CO_2 does, and the solubility of CFCs is much more sensitive to changes in temperature than the solubility of CO_2 is. These two factors increase the ratio of CFC to anthropogenic CO_2 concentrations in the Southern Ocean.
20. W. S. Broecker, S. Sutherland, T.-H Peng, *Science* **286**, 1132 (1999).
21. These conclusions are echoed by a study showing deep convection to play a subordinate role in tracer transport in the North Atlantic [A. J. Watson *et al.*, *Nature* **401**, 902 (1999)].

22. We thank N. Gruber, R. M. Key, and C. L. Sabine for their insightful papers and access to the data underlying them. K.C. was supported by the NASA Oceanography Program and the U.S. Department of Energy Center for Research on Ocean Carbon Sequestration. P.B.D. was supported by the Lawrence Livermore National Laboratory Laboratory Directed Research and Development program.

15 July 1999; accepted 2 December 1999

Nanotube Molecular Wires as Chemical Sensors

Jing Kong,[1]* Nathan R. Franklin,[1]* Chongwu Zhou,[1] Michael G. Chapline,[1] Shu Peng,[2] Kyeongjae Cho,[2] Hongjie Dai[1]†

Chemical sensors based on individual single-walled carbon nanotubes (SWNTs) are demonstrated. Upon exposure to gaseous molecules such as NO_2 or NH_3, the electrical resistance of a semiconducting SWNT is found to dramatically increase or decrease. This serves as the basis for nanotube molecular sensors. The nanotube sensors exhibit a fast response and a substantially higher sensitivity than that of existing solid-state sensors at room temperature. Sensor reversibility is achieved by slow recovery under ambient conditions or by heating to high temperatures. The interactions between molecular species and SWNTs and the mechanisms of molecular sensing with nanotube molecular wires are investigated.

Carbon nanotubes are molecular-scale wires with high mechanical stiffness and strength. A SWNT can be metallic, semiconducting, or semimetallic, depending on its chirality (*1*). Utilization of these properties has led to applications of individual nanotubes or ensembles of nanotubes as scanning probes (*2, 3*), electron field emission sources (*4*), actuators (*5*), and nanoelectronic devices (*6*). Here, we report the realization of individual semiconducting-SWNT (S-SWNT)–based chemical sensors capable of detecting small concentrations of toxic gas molecules.

Sensing gas molecules is critical to environmental monitoring, control of chemical processes, space missions, and agricultural and medical applications (*7*). The detection of NO_2, for instance, is important to monitoring environmental pollution resulting from combustion or automotive emissions (*8*). Detection of NH_3 is needed in industrial, medical, and living environments (*9*). Existing electrical sensor materials include semicon-

[1]Department of Chemistry, [2]Department of Mechanical Engineering, Stanford University, Stanford, CA 94305, USA.

*These authors contributed equally to this work.
†To whom correspondence should be addressed. E-mail: hdai@chem.stanford.edu